Supporting Information

Polymeric α-Tetrasubstituted Co^{II}-phthalocyanine Catalyst for Stable and Selective Electrochemical Carbon Dioxide Reduction

Kornkamol Mangmoon,[a] Permsak Chairat,[a] Yijiao Jiang,[b] Poobodin Mano,[c] Supawadee Namuangruk,[c] and Patchanita Thamyongkit*[a]

[a] K. Mangmoon, P. Chairat, Prof. P. Thamyongkit
Department of Chemistry, Faculty of Science, Chulalongkorn University, Bangkok 10330, Thailand
E-mail: patchanita.v@chula.ac.th
[b] Y. Jiang
School of Engineering, Macquarie University, NSW, 2109, Sydney, Australia
[c] S. Namuangruk
National Nanotechnology Center (NANOTEC)
National Science and Technology Development Agency (NSTDA)
Pathum Thani, 12120, Thailand
* Corresponding author E-mail address: patchanita.v@chula.ac.th

Table of Contents

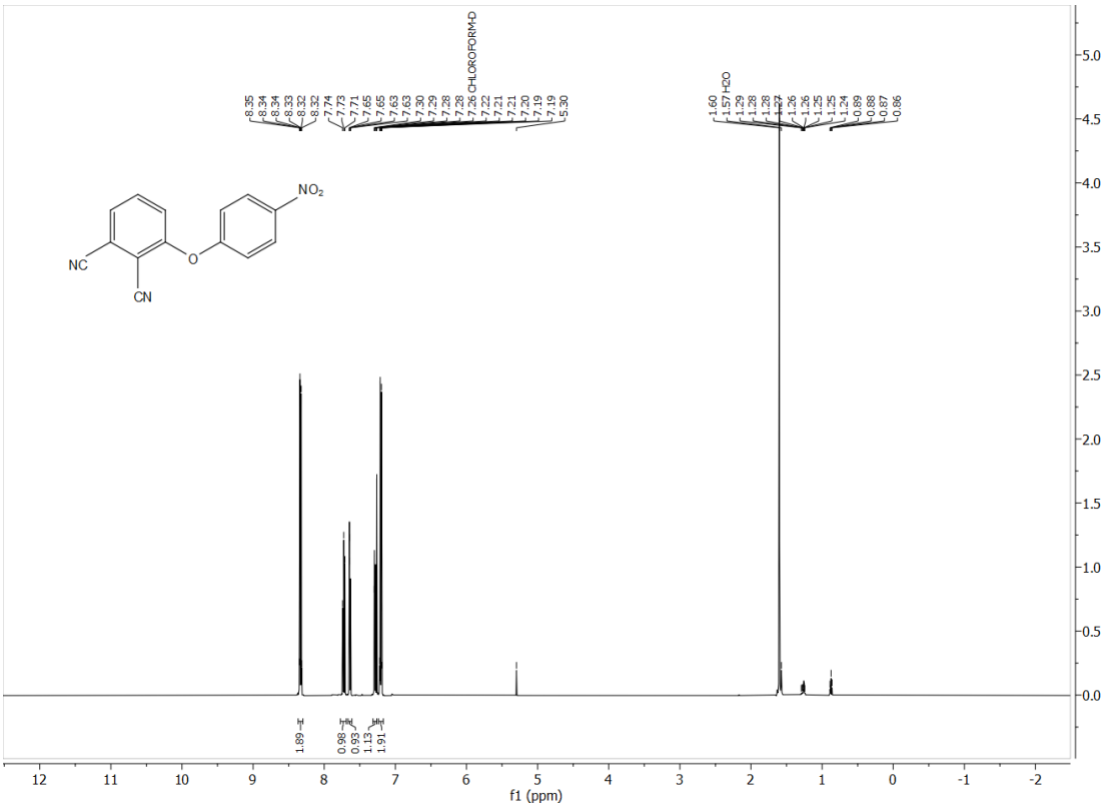

Fig. S1. A ^{1}H NMR spectrum of compound **1** in $CDCl_3$

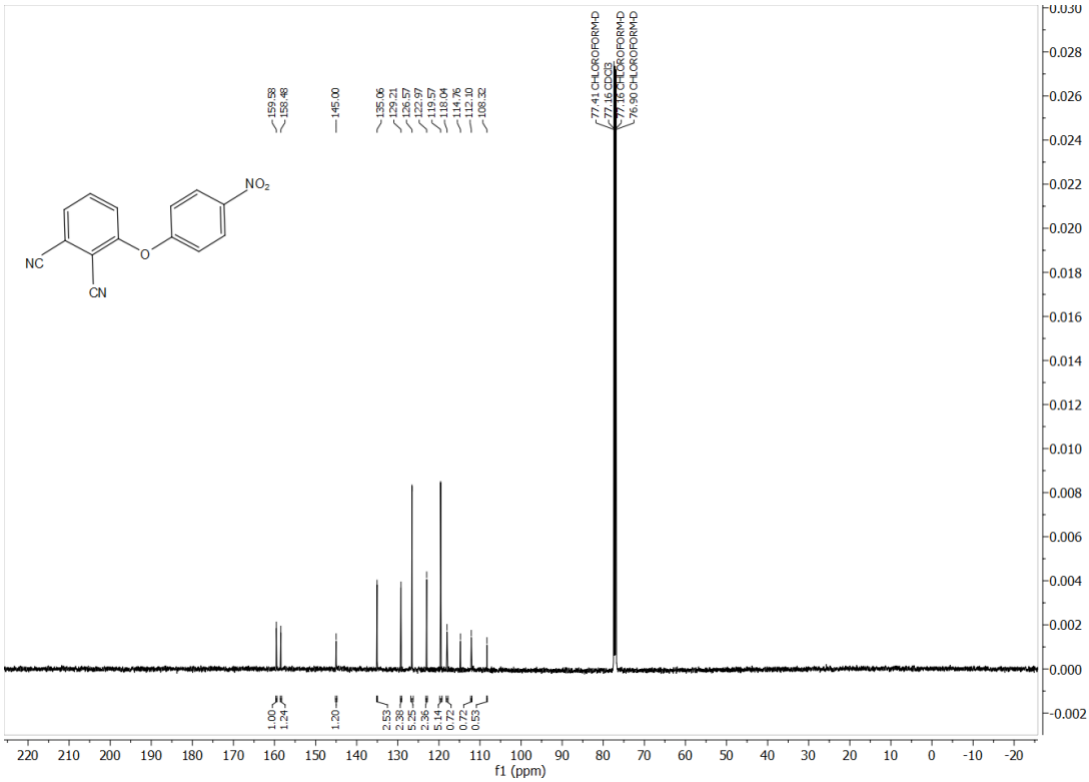

Fig. S2. A ^{13}C NMR spectrum of compound **1** in $CDCl_3$

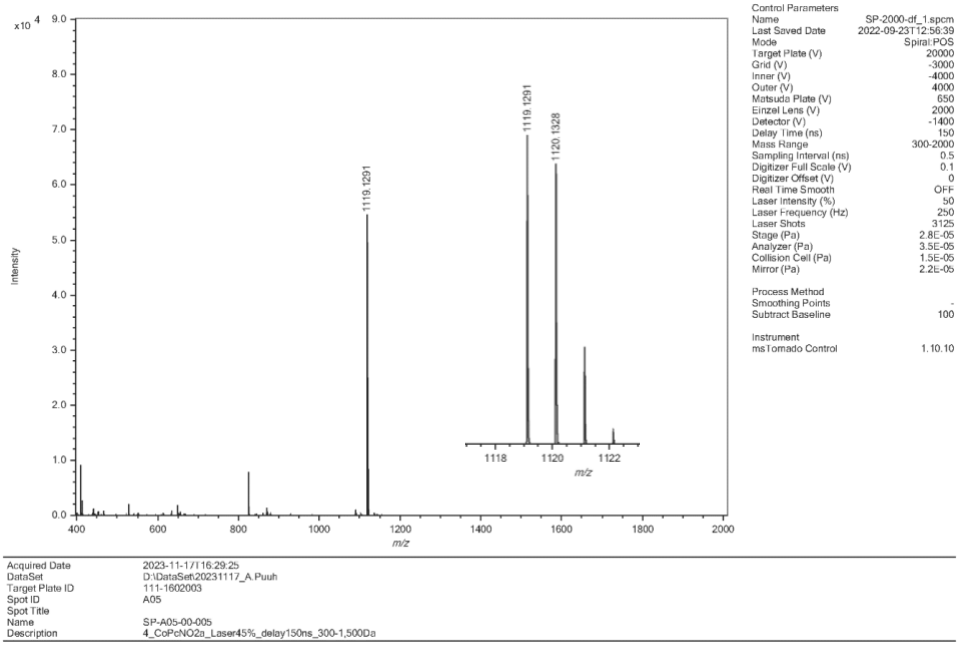

Fig. S3. An HR-MALDI-TOF mass spectrum and an isotopic pattern of a molecular ion peak of **CoPc-2α**

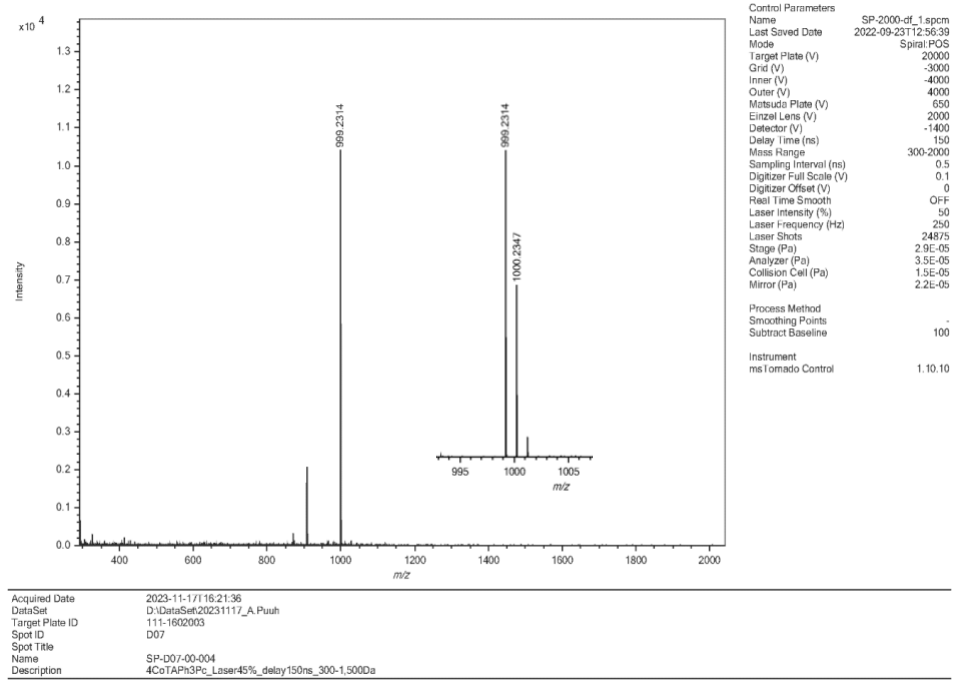

Fig. S4. An HR-MALDI-TOF mass spectrum and an isotopic pattern of a molecular ion peak of **CoPc-1α**

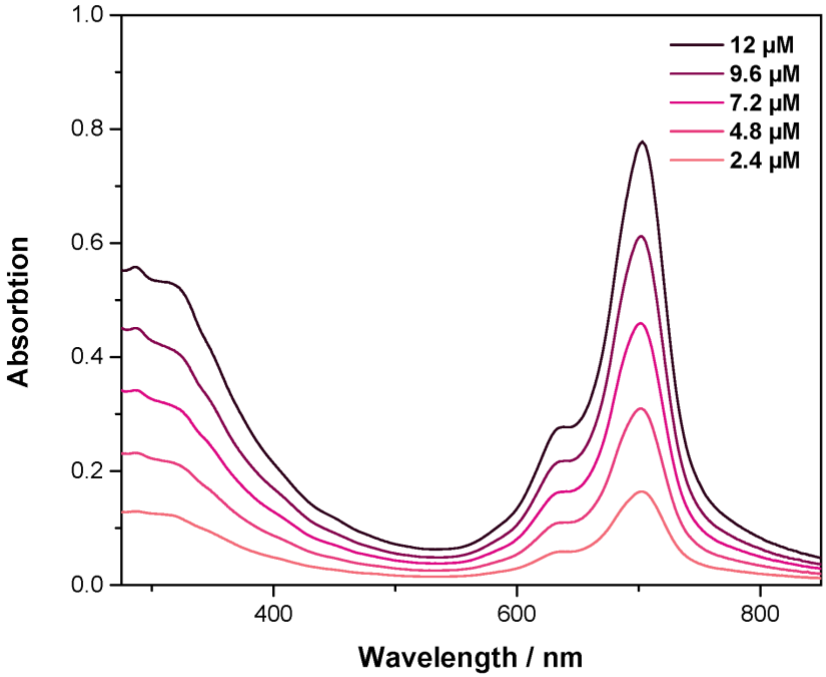

Fig. S5. Absorption spectra of **CoPc-1α** in DMF

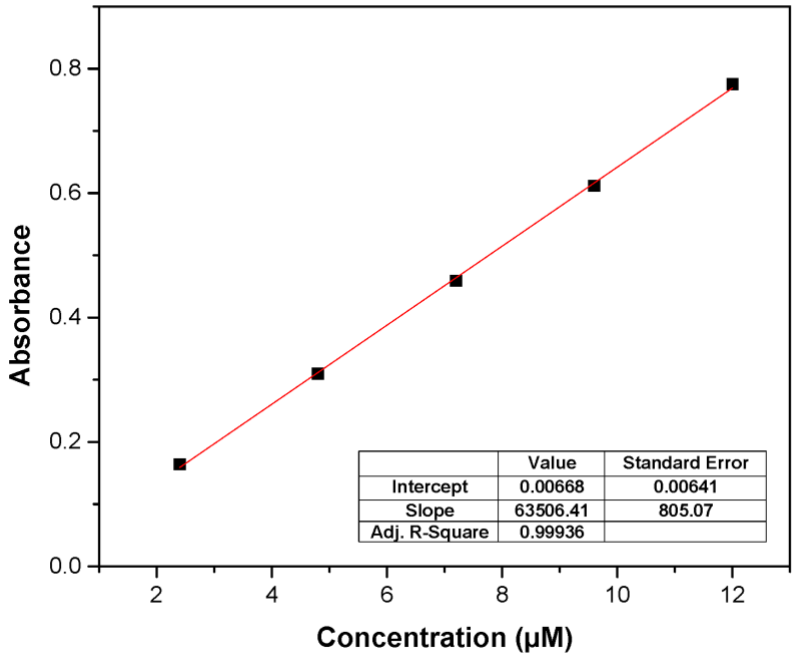

Fig. S6. Calibration curve for absorption at 702 nm of **CoPc-1α** in DMF

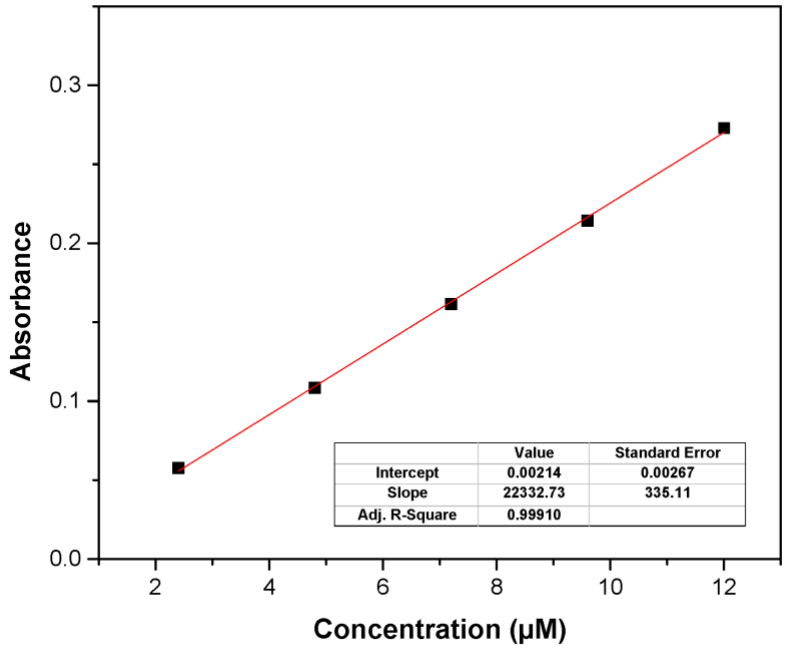

Fig. S7. Calibration curve for absorption at 633 nm of **CoPc-1α** in DMF

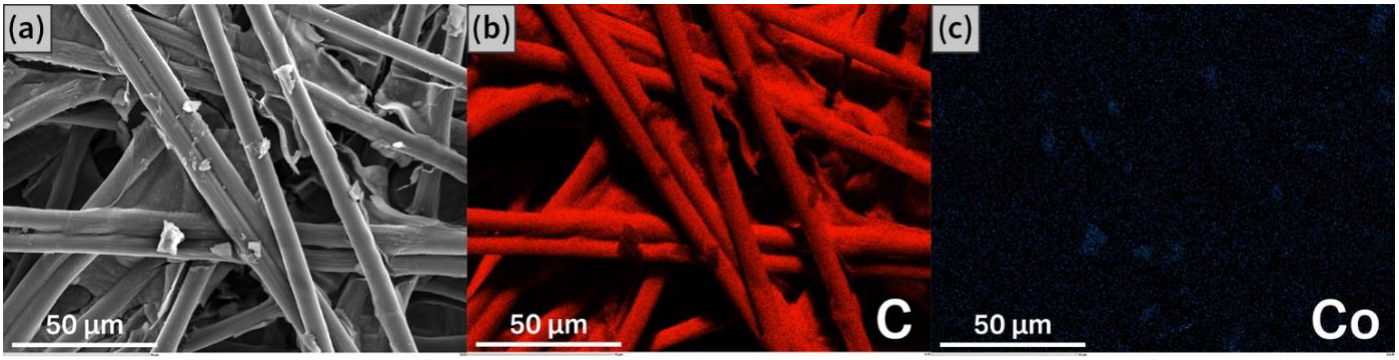

Fig. S8. SEM image of (a) **p(CoPc-1α)**/CP, and EDS mapping of (b) carbon and (c) cobalt atoms.

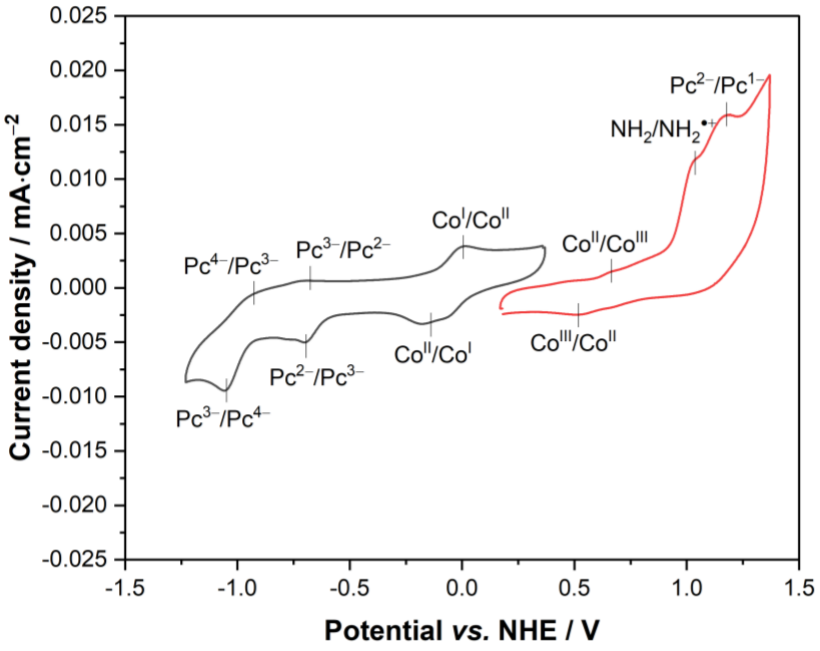

Fig. S9. Cyclic voltammograms of a **CoPc-1*α*** solution in DMF

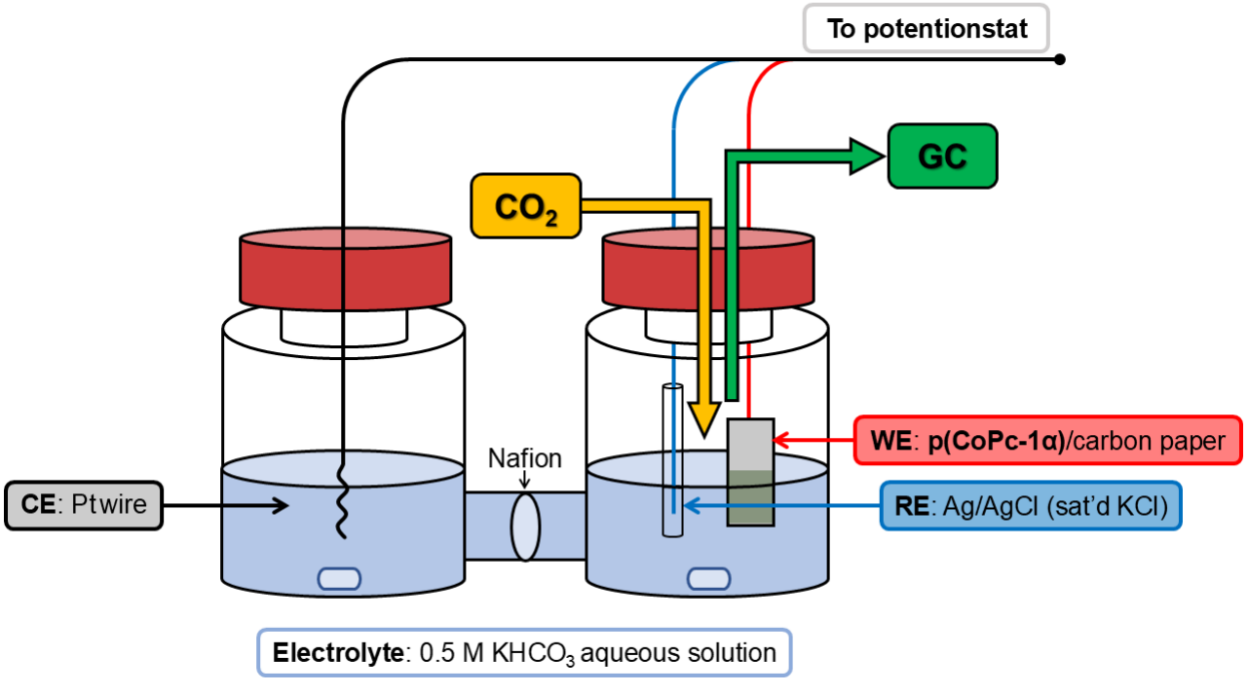

Fig. S10. An H-type electrochemical setup

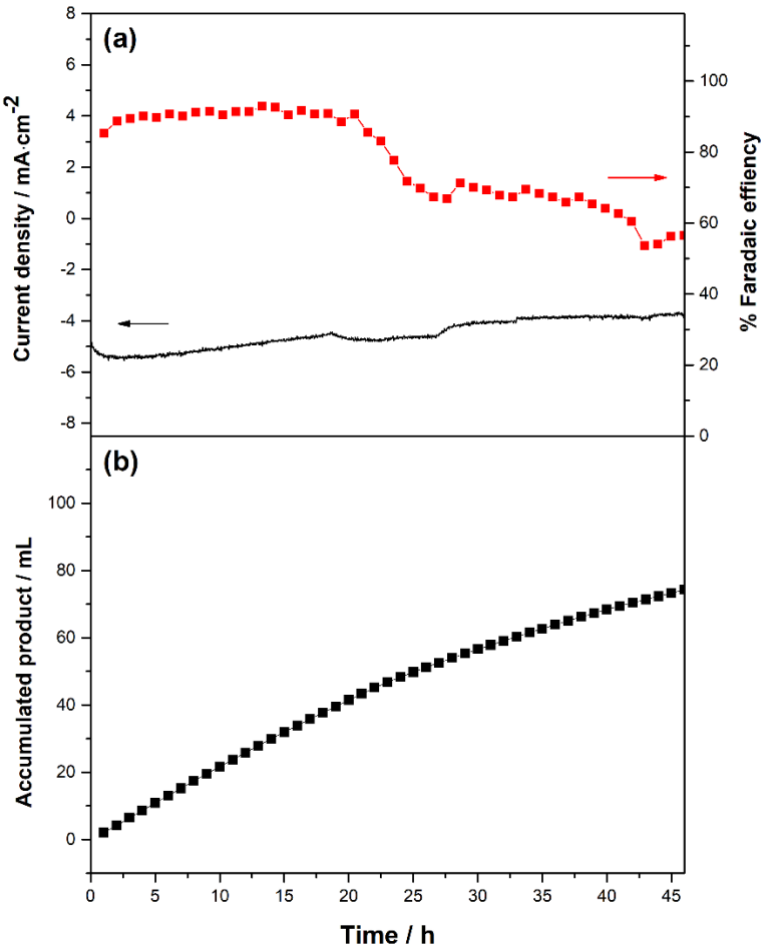

Fig. S11. (a) chronoamperometric responses with % FE_{CO} and (b) accumulated amount of CO recorded over 45 h at –1.20 V *vs.* NHE for the **p(CoPc-1α)**-catalyzed CO_2RR in the H-cell.

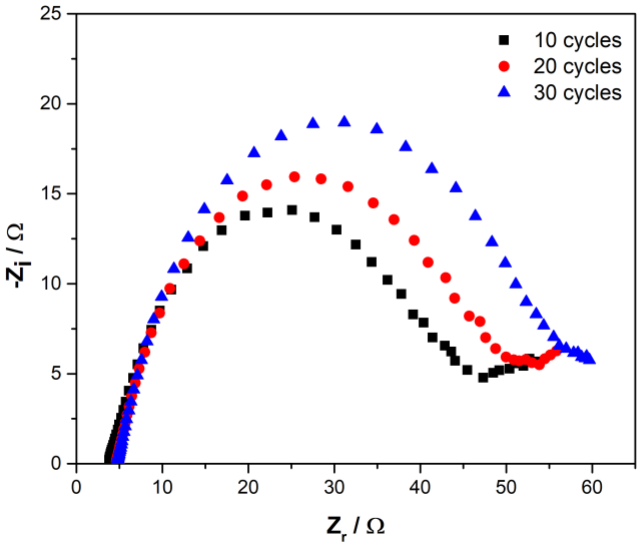

Fig. S12. Nyquist plots of faradaic impedance for the **p(CoPc-1α)** films obtained from the electropolymerization of **CoPc-1α** on the CP for 10 cycles (black squares), 20 cycles (red circles) and 30 cycles (blue triangles). The measurements were performed at –0.95 V *vs.* NHE in a CO_2-saturated 0.5 M $KHCO_3$ aqueous solution in the frequency range of 0.1 Hz to 100000 Hz.

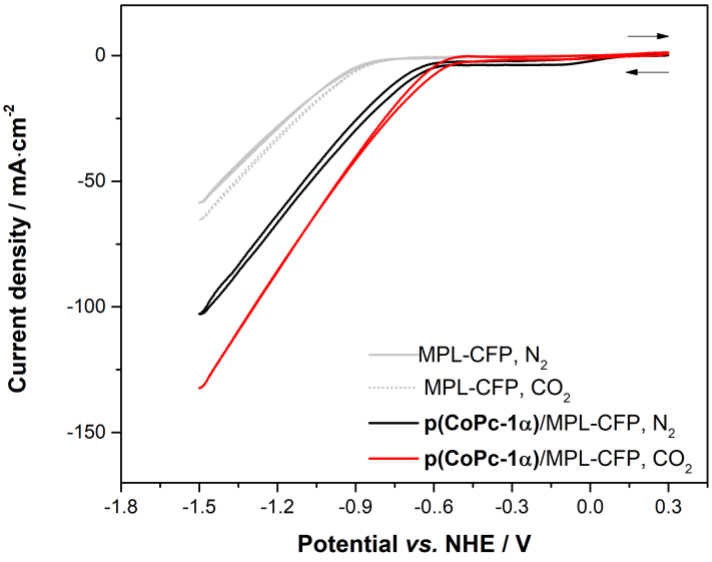

Fig. S13. Cyclic voltammograms of **p(CoPc-1α)**/MPL-CFP under N_2- (black solid line) and CO_2-saturated (red solid line) conditions, compared with those of a bare MPL-CFP under the N_2- (grey solid line) and CO_2-saturated (grey dashed line) conditions recorded in a 1.0 M $KHCO_3$ solution at a scan rate of 50 $mV \cdot s^{-1}$.

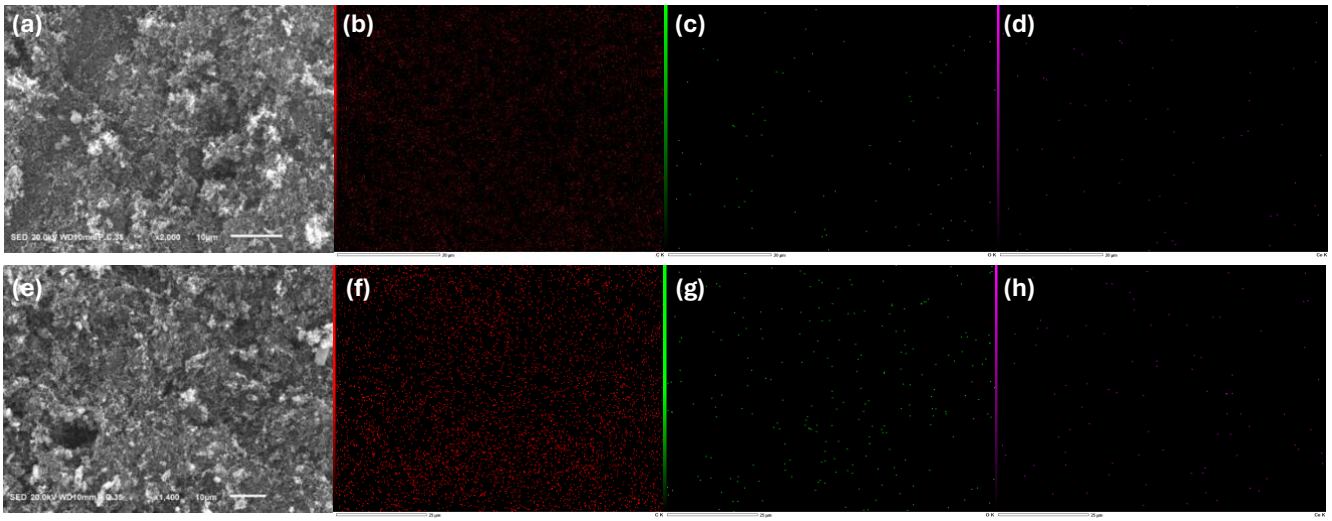

Fig. S14. (a) SEM image and EDS mapping of (b) carbon and (c) oxygen and (d) cobalt atoms of **p(CoPc-1α)**/MPL-CFP before electrolysis, and (e) SEM image and EDS mapping of (f) carbon and (g) oxygen and (h) cobalt atoms of **p(CoPc-1α)**/MPL-CFP after electrolysis.

Modelling of CoPc-1α and p(CoPc-1α)

The optimized structures of **CoPc-1α** and **p(CoPc-1α)** are shown in **Fig. S13a-b**. Here, the polymer form has lattice size of 22.30 Å in both x- and y-direction. To model the adsorption on the graphene substrate, the orthorhombic graphene cell in (16,9,1) and (9,5,1) size of supercell were prepared for the substrate for **CoPc-1α** and **p(CoPc-1α)** (**Fig. S13c-d**). The lattice mismatch in polymer model was –4.5% and –0.7% in x and y direction of **p(CoPc-1α)**, respectively.

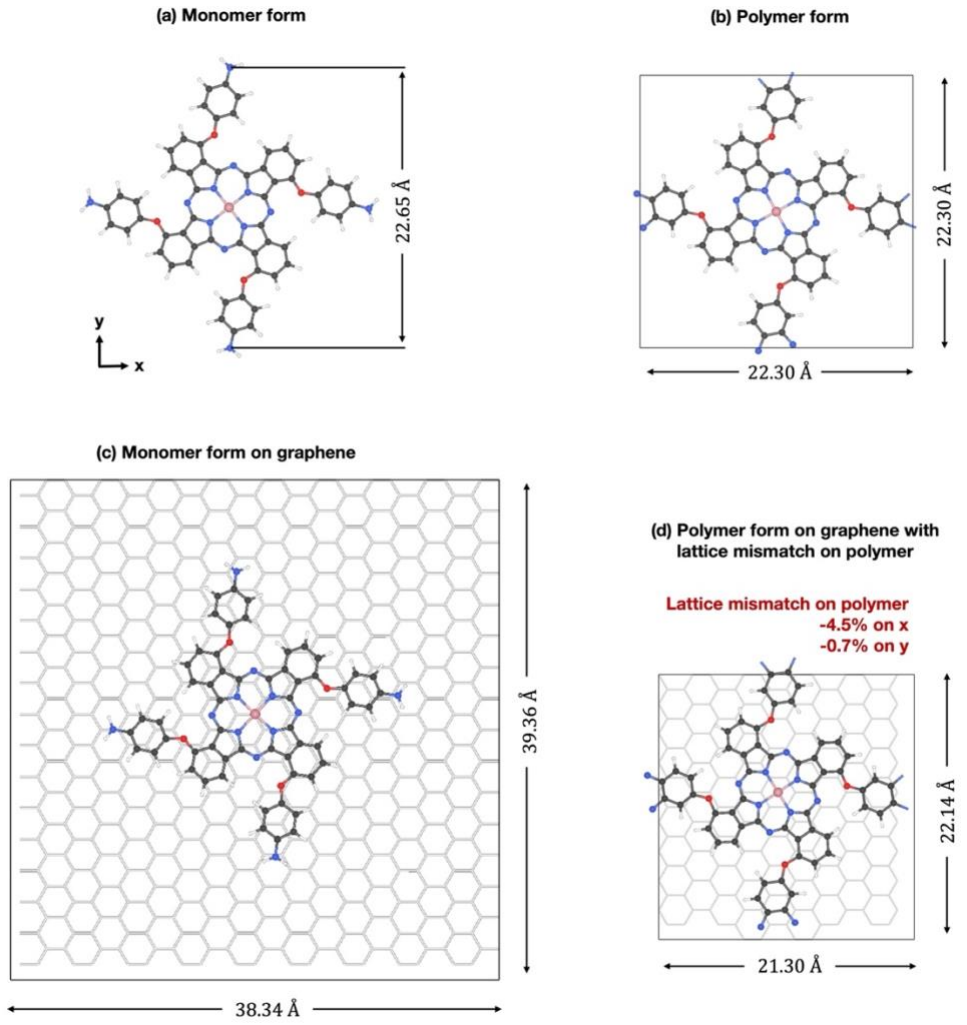

Fig. S15. The optimized structure of **CoPc-1** (a) and **p(CoPc-1α)** (b). The simulation box for **CoPc-1** (c) and **p(CoPc-1α)** (d) stacked on the graphene substrate.

Modelling of deposition of CoPc-1α on the substrate

The first layer deposition of the monolayer of **CoPc-1α** on the graphene substrate was investigated. As shown in **Fig. S16**, the stacking configurations where the Co center is located on atop (T), bridge (B) and hollow (H) site of sp^2-C of graphene were investigated. The orientation angle (θ) of each stacking pattern was compared at $\theta = 0°$, 15°,30°, 45°, 60° and 75°. The most stable configuration was found to be the hollow site at $\theta = 75°$ (denoted as H75) with adsorption energy of 0.39 eV. Therefore, the subsequent investigation will be conducted using this stacking order.

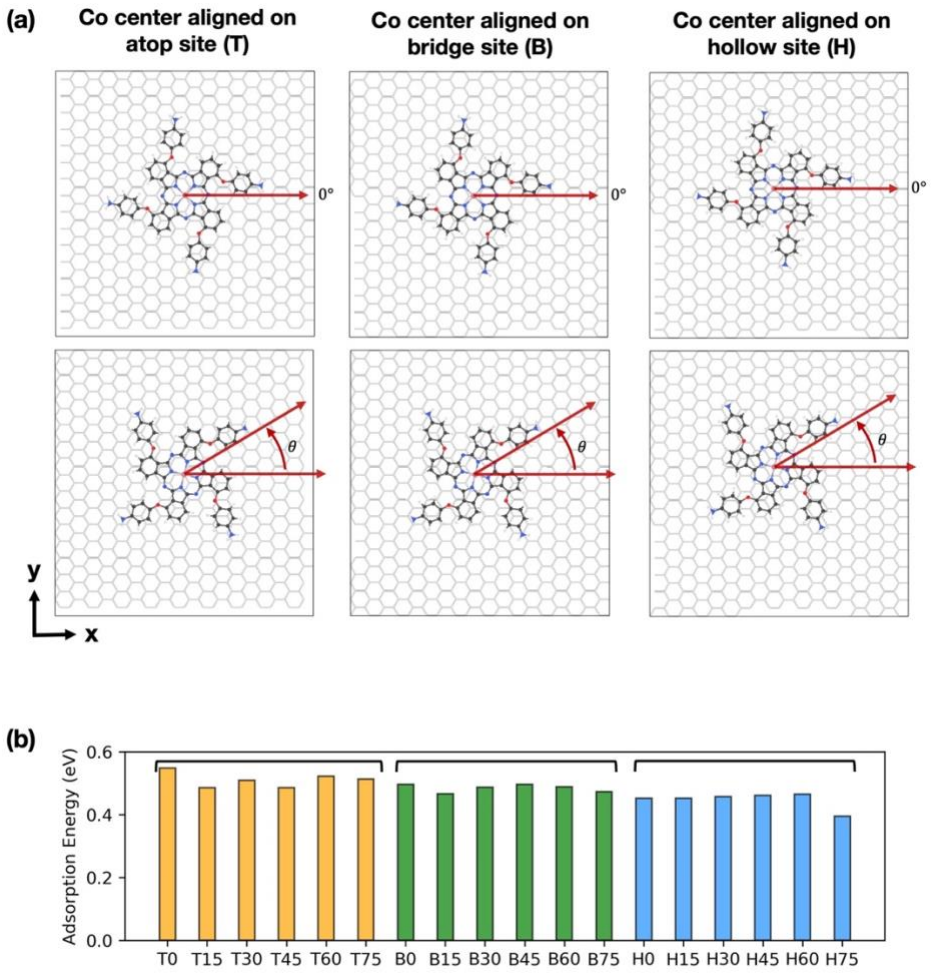

Fig. S16. (a) Stacking configuration of **CoPc-1α** on the graphene substrate where a Co center aligned on atop, bridge and hollow sites of sp^2-C of graphene. The orientation θ of each stacking pattern was probed by rotating each configuration by 0°, 15°,30°, 45°, 60° and 75° (b) Adsorption energy of each stacking pattern for first layer deposition.

To discuss charge transfer between neighboring **CoPc-1α** layers, we deposited the second layer on the first layer (H75). The stacking order of the second layer was considered as shown in **Fig. S17**. The charge density change due to the stacking will be calculated for all possibilities to provide the possible range of electron accumulation and electron depletion.

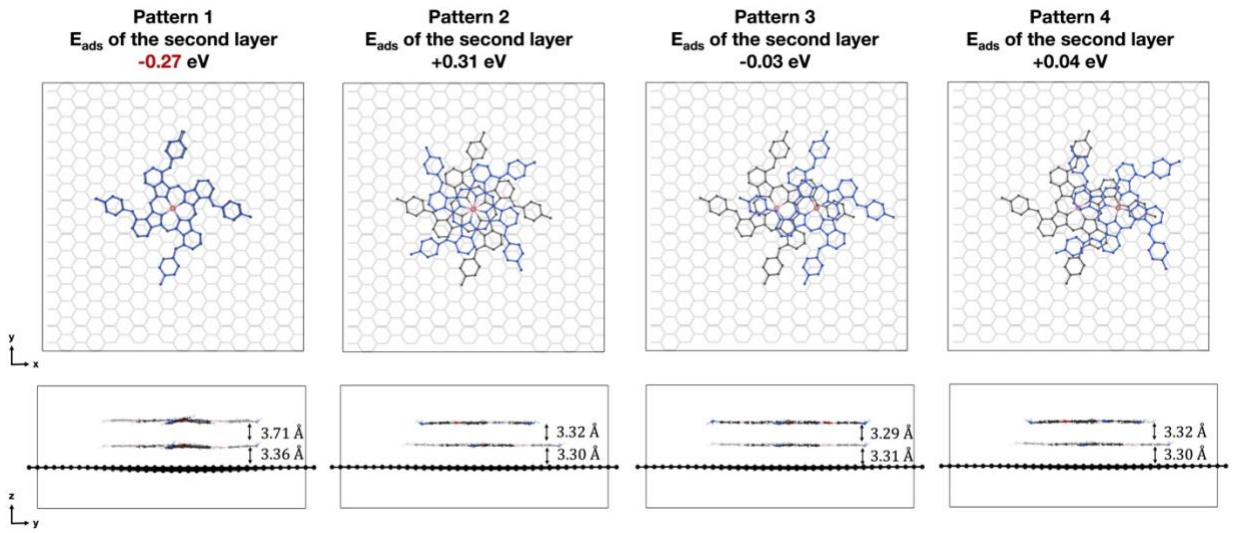

Fig. S17. Stacking configuration of **CoPc-1α** at the second layer (blue) on the graphene substrate where the first layer (black) aligned on atop site with orientation angle of 75°. The deposition of second layer was considered in 4 different possibilities.

Modelling of deposition of p(CoPc-1α) on the substrate

The first layer deposition of **p(CoPc-1α)** on the graphene substrate was investigated. As seen in the monomer case, the stacking configurations where the Co center is located on atop (T), bridge (B) and hollow (H) site of sp^2-C of graphene were investigated (**Fig. S18**). Due to the limitation of periodic constraint of the model, the orientation dependence was ignored. Overall, the binding energy between **p(CoPc-1α)** and graphene was confirmed to be positive, showing **p(CoPc-1α)** weakly bound on the substrate.

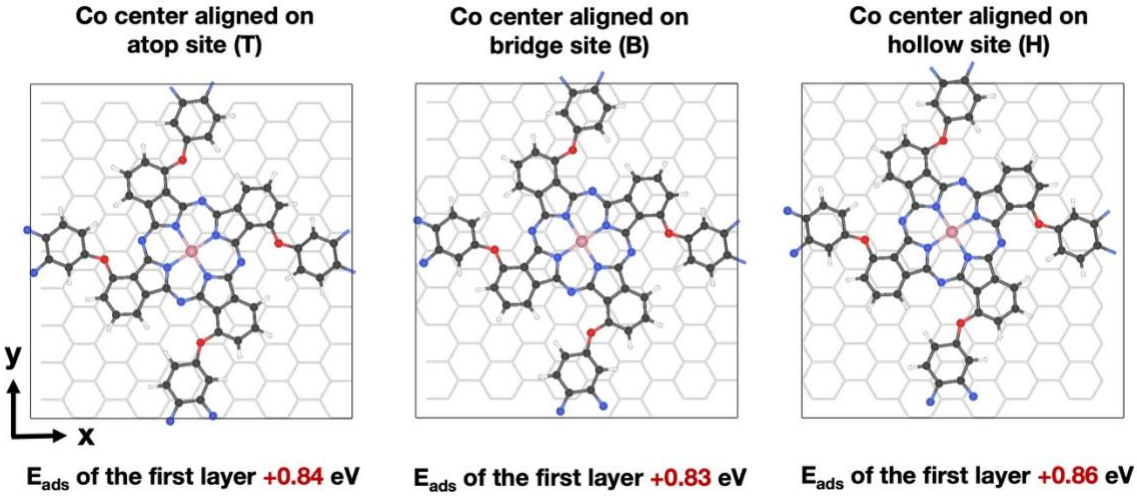

Fig. S18. Stacking configuration of **p(CoPc-1α)** on the graphene substrate where the Co center aligned on atop, bridge and hollow site of sp^2-C of graphene. Due to the limitation of periodic constraint in the model, the orientation dependence was ignored.

To discuss charge transfer between neighboring **p(CoPc-1α)** layers, we deposited the second layer on the first one. The stacking order of the second layer was considered in 3 possibilities as

shown in **Fig. S19**. Although the most energetically favorable configuration was found to be pattern 3 with positive adsorption energy of 0.21 eV, the charge density change due to the stacking will be calculated for all possibilities to provide the possible range of electron accumulation and electron depletion.

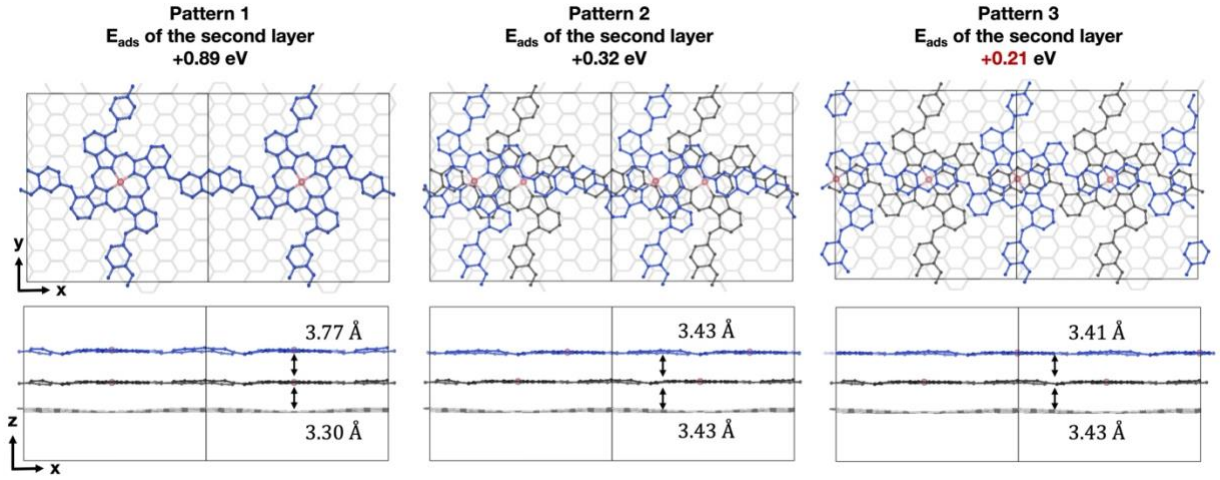

Fig. S19. Stacking configuration of **p(CoPc-1α)** at the second layer (blue) on the graphene substrate where the first layer (black) aligned on bridge site. The deposition of the second layer was considered in 3 different possibilities.

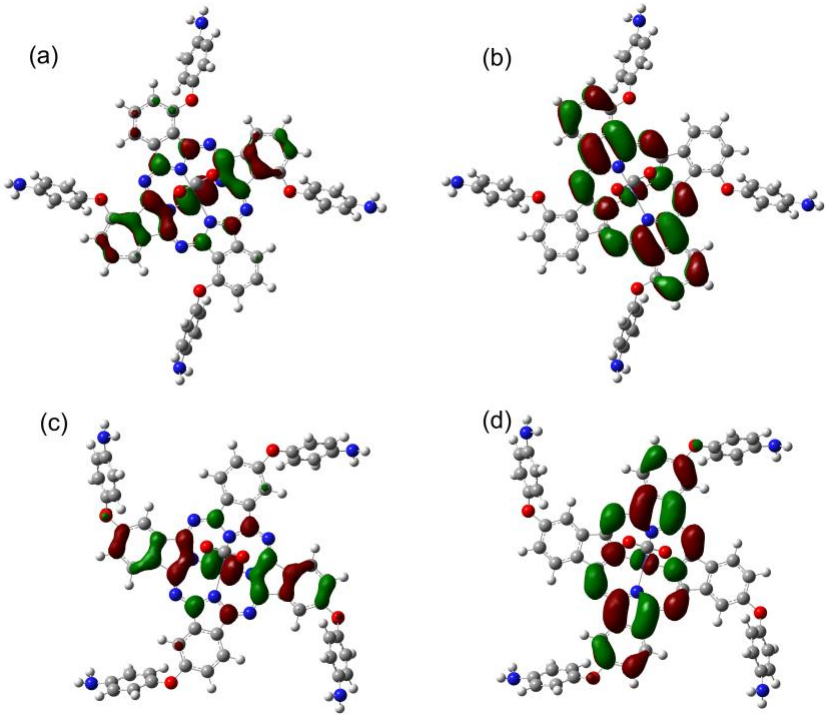

Fig. S20. (a) HOMO, (b) LUMO orbitals of CO_2 adsorbed on the **CoPc-1α** molecule and (c) HOMO, (d) LUMO of CO_2 adsorbed on the **CoPc-1β** molecule.

Table S1. Assignment of ATR-FTIR spectra of **CoPc-2α**, **CoPc-1α** and **p(CoPc-1α)**/Au-glass

Wavenumber / cm^{-1}			**Assignment**	**Reference**
CoPc-2α	**CoPc-1α**	**p(CoPc-1α)**		
738	740		δ_{C-H} (out-of-plane)	[43]
		752	out-of-plane vibrations of C-H groups in phenazines	[51]
		812	skeletal deformations of phenazine ring system	[51]
835	836	854	$C\text{-}H_{Ar\text{-}O\text{-}Ar}$ rocking	[44]
976	976	983	Benzene totally symmetric vibration	[43]
		983	C-H in-plane deformation bands	[51]
	1084	1090	C-O-C stretching and δ_{C-H} (in-plane)	[43,45,46]
		1090	C-H in-plane deformation bands	[51]
1107	1127	1135	Isoindole totally symmetric vibration	[43]
		1135	C-H in-plane deformation bands	[51]
		1204	C-H in-plane deformation bands	[51]
1236	1237	1251	$C_{aromatic}$-O-C stretching	[45,47]
1326	1325	1331	C-C stretching in isoindole and υ (pyrrole)	[43,48]
	1408	1410	C-C stretching in isoindole, and vibrations of pyrrole fragment and nitrogen mesoatoms	[43,48]
1491	1500	1507	υ (-N=)	[43]
1586	1589	1589	υ (C=C)	[43]
		2943	υ (C-H)	[43]
	3210		N-H stretching of primary amino group	[49]
	3324		N-H stretching of primary amino group	[49]
		3376	N-H stretching of secondary amino group	[50]

Table S2. Assignment of Raman spectra of **CoPc-1α**/CP and **p(CoPc-1α)**/CP.

Raman shift/ cm^{-1}		**Assignment**	**Reference**
CoPc-1α	**p(CoPc-1α)**		
754	754	Co-N stretching coupled with pyrrole expanding	[52]
1083	1083	C-H in-plane bending	[53]
1278	1278	C-H in-plane bending	[53]
1340	1340	Co-N stretching coupled with C-H in-plane bending, and isoindole stretching	[52]
1349	1349	C_β-C_β, C_α-C_β-C_β, C_γ-C_δ, and C_β-C_γ stretching vibration of the pyrrole group	[54]
1426	1426	C-N_m-C stretching, pyrrole expending and C-H in-plane bending	[55]
1462	1462	C-H in-plane bending and C_β-C_β stretching	[55]
1539	1539	C-N_m-C bridges stretching and pyrrole expanding coupled with C-H vibrations	[52]

Table S3. Co^{II} content on substrates determined by ICP-OES

Substrate types	Co^{II} content on substrates (μmol·cm^{-2})
Carbon paper	0.052
MPL-CFP	0.061

Calculations of $FE_{CO\ or\ H_2}$, TON and TOF

$$FE_{CO\ or\ H_2} = \frac{Z \times n \times F}{i_{total}} \times 100\%$$

$$Turnover\ number\ (TON) = \frac{mole\ of\ products}{mole\ of\ catalysts}$$

$$Turnover\ frequency\ (TOF) = \frac{TON}{time\ (s)}$$

Z number of electrons required to obtain product
n number of moles of the product
R gas constant, 8.314 J K^{-1} mol^{-1}
T temperature, 298.15 K
F Faraday's constant, 96485 C mol^{-1}
P pressure, 101325 Pa

Table S4. Comparison of catalytic performance of **p(CoPc-1α)**/CFP with selected reported CoPc-based catalysts for ECO_2R in the aqueous media.

Catalyst	Electrolyte	Cell type	Potential / V *vs.* NHE[a]	J / $mA \cdot cm^{-2}$	FE_{CO} / %	TOF_{CO} / s^{-1}	Stability / h	Ref.
p(CoPc-1α)	0.5 M $KHCO_3$	H-cell	–1.15	3.8	97	0.37	45	This work
	1.0 M $KHCO_3$	Flow cell	–1.54	151	98	13	42	
p(CoPc-1β)	0.5 M $KHCO_3$	H-cell	–1.19	5.9	94	1.1	120	[25]
p-CoTAPc	1 M $KHCO_3$	Flow cell	–1.60[a]	153 ±10	93 ±9	~140	41	[24]
p(CoPc-1)	0.5 M $KHCO_3$	H-cell	–1.09	~2	94	0.29	24	[23]
CoPc-PI-COF-1	0.5 M $KHCO_3$	H-cell	–1.13[a]	9.4	93	2.2	40	[60]
	1.0 M KOH	Flow cell	–0.93[a]	44	95	n.a.[b]	n.a.[b]	
CoPc-PI-COF-2	0.5 M $KHCO_3$	H-cell	–1.13[a]	6.2	95	1.9	n.a.[b]	
CoPc-PI-COF-3	0.5 M $KHCO_3$	H-cell	–1.23[a]	~31.7	96	0.6	20	[61]

[a] Values were estimated from the reported data in the RHE scale by using equation $E_{RHE} = E_{NHE} + 0.059pH$

[b] Data was not available.